Received: 10 April 2023 | Revised: 22 July 2023 | Accepted: 24 July 2023

DOI: 10.1002/psc.3535

RESEARCH ARTICLE

Journal of PeptideScience WILEY

Designed novel nuclear localizing anticancer peptide targets p53 negative regulator MDM2 protein

Nabanita Mukherjee[1] | Debmalya Bhunia[2] | Prabir Kumar Garai[3] | Prasenjit Mondal[4] | Surajit Barman[5] | Surajit Ghosh[1,3]

[1]Smart Healthcare, Interdisciplinary Research Platform, Indian Institute of Technology Jodhpur, Karwar, Rajasthan, India

[2]Department of Chemistry & Biochemistry, The Ohio State University, Columbus, Ohio, USA

[3]Department of Bioscience & Bioengineering, Indian Institute of Technology Jodhpur, Karwar, Rajasthan, India

[4]Genetics and Aging Research Unit, McCance Center for Brain Health, MassGeneral Institute for Neurodegenerative Disease, Department of Neurology, Massachusetts General Hospital, Harvard Medical School, Charlestown, Massachusetts, USA

[5]Department of Chemical Sciences and Centre for Advanced Functional Materials, Indian Institute of Science Education and Research, Kolkata, West Bengal, India

Correspondence
Surajit Ghosh, Department of Bioscience & Bioengineering, Smart Healthcare, Interdisciplinary Research Platform, Indian Institute of Technology Jodhpur, NH 62, Surpura Bypass Road, Karwar, Rajasthan 342037, India.
Email: sghosh@iitj.ac.in; sghosh@iicb.res.in

Funding information
Science and Engineering Research Board, Grant/Award Number: STR/2020/000048

Intracellular protein–protein interactions provide a major therapeutic target for the development of peptide-based anticancer therapeutic agents. MDM2 is the 491-residue protein encoded by the *MDM2* oncogene. Being a ubiquitin-protein ligase, MDM2 represses the transcription ability of the tumor suppressor p53 by proteasome-mediated degradation. Under typical cellular circumstances, a sustained p53 expression level is maintained by negative regulation of MDM2, whereas under stress conditions, this is alleviated to increase the p53 level. Modulation of MDM2-p53 interaction via fabrication of an MDM2-interacting peptide could be a useful strategy to inhibit subsequent proteasomal degradation of p53 and initiation of p53 signaling leading to the initiation of p53-mediated apoptosis of tumor cells. Here, in this research work, a novel anticancer peptide mPNC-NLS targeting the nucleus and the MDM2 protein (p53 negative regulator) was designed to promote the p53 protein activity for the prevention of cancer. It induces effective apoptosis in both A549 and U87 cells and remains non-cytotoxic to normal lung fibroblast cells (WI38). Further, immunocytochemistry and Western blot results confirm that the designed mPNC-NLS peptide induces the apoptotic death of lung cancer cells via activation of p53 and p21 proteins and remarkably stifled the in vitro growth of 3D multicellular spheroids composed of A549 cells.

KEYWORDS
3D spheroid, HDM2/MDM2, nuclear localizing, p53, protein–protein interaction

1 | INTRODUCTION

The tumor suppressor gene *p53*, known as the guardian of the genome, plays a significant role in cell survival and maintenance.[1,2] MDM2 is a p53-specific ubiquitin E3 ligase and thus promotes subsequent proteasome mediated degradation of p53. Principally, it is a cellular stress detector that initiates cell cycle arrest, and apoptosis in retaliation to various stresses, including DNA damage, hyperproliferative signals, hypoxia condition, oxidative stress, ribonucleotide depletion, and nutrient starvation.[1–4] The ordinance of multiple p53 stress responses is mediated through the MDM2 protein (human double minute 2 gene also known as HDM2).[4,5] It is recognized that MDM2, a negative regulator of p53 protein, significantly controls the activity of p53 protein. Downregulation of *MDM2* makes p53 activated and cancer cells undergo apoptotic death or repair.[6] Therefore, disruption of p53/MDM2, protein–protein interaction (PPI), maybe a smarter perspective for the development of targeted anticancer therapy as it enhances the likelihood to trigger the wild-type p53 responsive genes in malignant cells. Therefore, significant targeted drug discovery efforts are directed toward blocking the p53-MDM2 interaction. So far various

Nabanita Mukherjee and Debmalya Bhunia contributed equally.

small molecules, metal complexes, and peptides have shown their anticancer potential via the modulation of various intercellular protein–protein interactions.[7–15] Among them, PNC27, an MDM2 targeting peptide, exhibited its significant anticancer activity.[16,17] It exhibits anticancer activity in different cancerous cells MIA-PaCa (human pancreatic cancer), MCF-7 (human breast cancer), A2058 (human melanoma), and Ag13145 cells (primary human fibroblasts) cells.[16] Yazdi et al. have designed the PNC27 peptide sequence (PPLSQETFSDLWKLL) attached with membrane residency peptide (MRP, KKWKMRRNQFWVKVQRG) to target the MDM2 protein that existed at the cell membrane.[16,17] However, this sequence is very long and often undergoes undesired activity due to poor interaction with the cancer cell membrane. To address this issue by increasing its effectivity as well as selectivity, here in this work, we have targeted the negative regulator of the p53 protein situated in the cell nucleus. Our main aim is to design a short MDM2 binding peptide attached to a nuclear localizing sequence (NLS) to target the negative regulator of p53 protein (MDM2) located at the cell nucleus (Scheme 1). To do this we have redesigned the PNC27 peptide by truncation approach and designed 11 amino acids containing modified PNC peptide (mPNC: QETFSDLWKLL). Further, we have attached a nuclear-localized motif (NLS: VQRKRQKLMP) with this truncated PNC peptide and established our final lead peptide mPNC-NLS (QETFSDLWKLLVQRKRQKLMP). Experimental data shows that mPNC-NLS can successfully localize itself into the nucleus of the cell and such rapid cellular internalization occurs via the endocytosis pathway. With a battery of further biological and biophysical experimental analysis, we have found that the designed mPNC-NLS effectively binds with the nuclear MDM2 protein and induce a significant apoptotic effect on human lung cancer cells (A549) via upregulation of p53 and p21. Apart from this, treatment of mPNC-NLS significantly inhibits the growth of multicellular 3D spheroid in in vitro experimental analysis.

2 | MATERIALS AND METHODS

2.1 | Chemicals

Rink amide AM solid support along with all the required amino acids were procured from Novabiochem in their respective Fmoc-protected form. The coupling agent HBTU (*O*-benzotriazol-1-yl-*N*,*N*,*N*′,*N*′-tetramethyluronium hexafluorophosphate) and activator base diisopropylethylamine (DIPEA) were purchased from Sigma Aldrich. Solvents like dimethylformamide (DMF), dichloromethane (DCM), and piperidine were purchased from Fisher Scientific. Phenol, diethyl ether, methanol, and trifluoroacetic acid (TFA) were purchased from Spectrochem. Ethanedithiol (EDT) and thioanisole were procured from Alfa-aesar. Molecular biology grade Triton X-100 and dimethyl sulfoxide (DMSO) was brought from Himedia. *N*,*N*′-Diisopropylcarbodiimide (DIC), 5(6)-carboxyfluorescein, 5-diphenyltetrazolium bromide (MTT), mouse double minute 2 (MDM2) protein, Dulbecco's modified Eagle's medium (DMEM), trypsin-EDTA solution, and formaldehyde solution (molecular biology grade) were procured from Sigma Aldrich. Fetal bovine serum (FBS) was purchased from Gibco, and Hoechst 33258 was purchased from Abcam. Antibiotic and antimycotic solutions were purchased from Invitrogen. Primary antibodies corresponding to p53 (mouse monoclonal, sc-393031), beta-actin (mouse monoclonal, C4: sc-47778), and p21 (Waf1/Cip1 (12D1) rabbit mAb: 2947) were purchased from

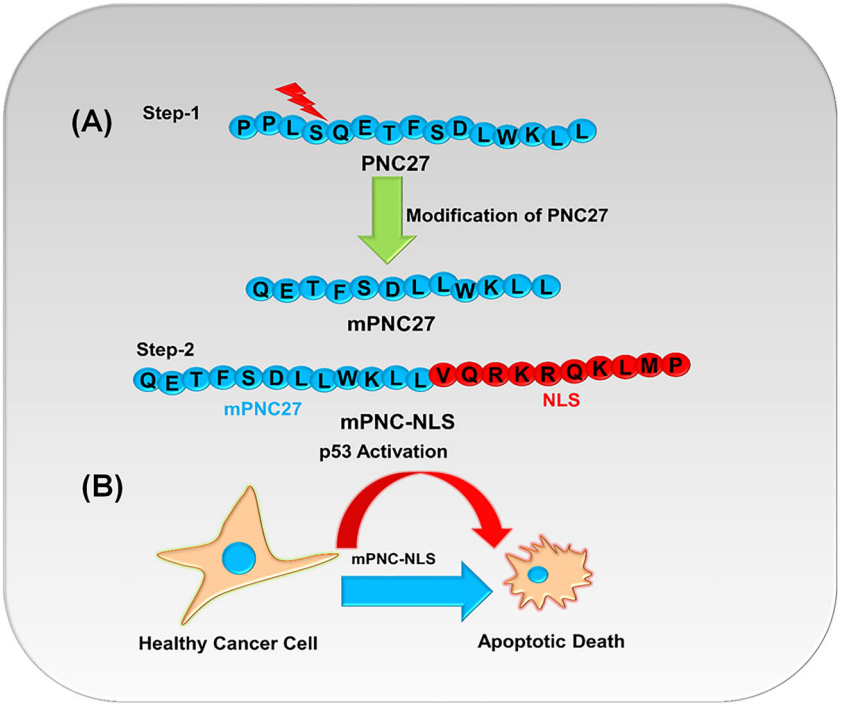

SCHEME 1 (A) Design and fabrication of a novel MDM2 targeting peptide mPNC-NLS having a nuclear localizing sequence (NLS). (B) Designed mPNC-NLS peptide targets and binds with MDM2 protein and activates p53 protein to induce apoptotic death of human lung carcinoma cells (A549).

Santa Cruz Biotechnology and CST respectively. The apoptosis analysis kit was purchased from Santa Cruz Biotechnology. Glass bottom confocal dishes were purchased from Ibidi. An HPLC system (Shimadzu) equipped with a C-18 reverse phase column was used to purify the synthesized peptides. After HPLC purification synthesized peptides were lyophilized in a Delvac freeze drier at −44°C. HPLC-quality water and acetonitrile were purchased from Alfa-Aeser.

2.2 | Cell culture study

A549 (human lung carcinoma), U87 (human glioblastoma), and WI38 (human normal lung fibroblast) cells were procured from National Centre for Cell Science (NCCS) Pune, India. Cells were cultured in DMEM culture media in combination with 10% fetal bovine serum along with kanamycin sulfate (110 mg/L), penicillin (50 units/mL), and streptomycin (50 μg/mL), using a CO_2 incubator (5%) at 37°C temperature.

2.3 | Solid-phase synthesis of truncated PNC27, nuclear-localization sequence (NLS), and mod. PNC27-NLS peptides including their 5,6-(carboxy) fluorescein-conjugated forms

For each peptide, 150 mg of Rink-Amide resin was weighed and swelled overnight in 1:1 DMF-DCM solvent at 4°C temperature. To perform coupling, each amino acid was taken in five equivalents excess along with the equal molecular equivalent of HBTU and 0.3 (M) DIPEA in 3 mL of DMF with an applied 40-watt microwave power for 5 min. Deprotection was performed using 20% piperidine in a CEM microwave-assisted peptide synthesizer using 40-watt microwave power for 3 min. DMF/DCM was used as a washing solvent. Synthesized peptides were subsequently cleaved by treating with a cleavage cocktail solution (92.5% trifluoroacetic acid (TFA), 2.5% milliQ water, 2.5% EDT and 2.5% phenol). A cleavage solution containing peptide-tethered resin was stirred for 4 h inside the hood. Then, excess trifluoroacetic acid was evaporated from the mixture by nitrogen flow and the remaining solution was added slowly to the ice-cold diethyl ether and stored at −20°C temperature overnight to ensure complete precipitation. The next day the peptide precipitation was separated by centrifugation at 5000 rpm for 5 min at 4°C. After lyophilization, the synthesized peptides were purified through C-18 reverse phase HPLC and molecular mass values were evaluated with the help of MALDI-TOF spectrometry. In a similar process, 5,6-carboxyfluorescein-conjugated peptides were synthesized and purified for further evaluation.

2.4 | Isothermal titration calorimetric analysis study

ITC analysis with MDM2 (50 μM) and peptide mPNC-NLS (500 μM) has been observed at 277 K using 0.1 mM PBS solution of each.[6] The resulting binding isotherm peaks shown in the upper box represent that ligand mPNC-NLS peptide solution was administrated into the MDM2 receptor protein solution. In the lower panels, the extent of absorbed heat due to recurring injections of peptide solution was plotted against the molar ratio of peptide to MDM2 protein (Figure 1). A standard nonlinear least squares regression binding model for one site binding has been applied to fit the data. The ITC plots for the binding of mPNC-NLS and MDM2 protein have been observed in the plot of power versus time explaining an endothermic binding. In order to carry out the control experiment (dilution), the mPNC-NLS peptide solution of the same concentration was administrated stepwise into the working buffer solvent. The absorbed heat of dilution for each injection was subtracted from the respective absorbed heat generated for MDM2 and mPNC-NLS association to calculate the corresponding heat change for the interaction reaction.[17,18]

Corresponding ITC data obtained for the binding of mPNC-NLS with MDM2 represents an association constant (K_a) of = (9.9 ± 2.2) × 10^4 M^{-1} along with a change in enthalpy (ΔH) of = (2070 ± 204) cal mol^{-1}, with a change in entropy (ΔS) = 30 kcal/mol and binding stoichiometry (N) = 5.9 ± 0.434. Gibbs energy change (ΔG°) and the subsequent entropic contribution for the binding ($T\Delta S^\circ$) were evaluated by using the relation: equation (1): $\Delta G^\circ = -RT \ln K_a$ and equation (2): $\Delta G^\circ = \Delta H^\circ - T\Delta S^\circ$ where T is the temperature in Kelvin and R represents the universal gas constant (1.9872041 cal mol^{-1} K^{-1}). The resultant negative Gibbs free energy change ($\Delta G^\circ = -6.4$ kcal/mol) implies an overall thermodynamically favorable binding process.

2.5 | Molecular docking study

A blind molecular docking study has been performed using AutoDock Vina software (version 1.1.2). A grid box of dimension 66 × 60 × 50 was made centered on the receptor (PDB ID: 1YCR)[19] MDM2 oncoprotein bound transactivation domain of p53 for docking with mPNC-NLS peptide.

2.6 | Fluorescence microscopy

A549 cells were treated with 5,6-carboxyfluorescein attached mPNC and mPNC-NLS peptides at 5-μM concentration for 6 h. After the end of the incubation period, treated cells were visualized under an inverted fluorescence microscope (Olympus IX83) at 40× magnification equipped with an ANDOR iXON3 camera.

2.7 | Cell viability assay of synthesized peptides

A549 (human lung carcinoma), U87 (human glioblastoma), and WI38 (normal lung fibroblast) cells were cultured in DMEM + 10% fetal bovine serum containing media supplemented with antibiotics and

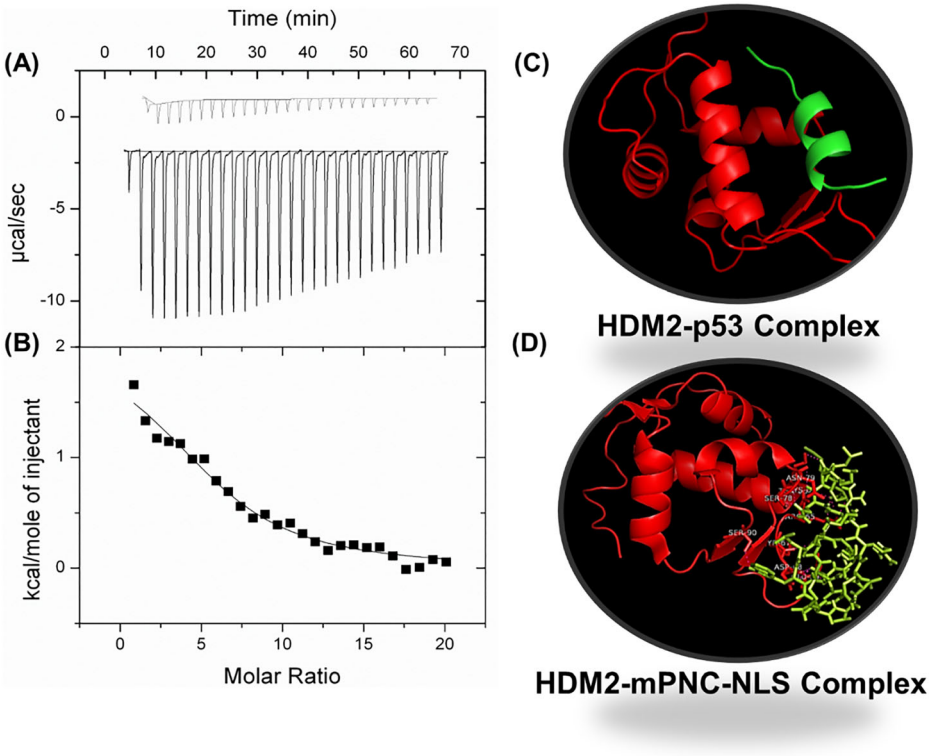

FIGURE 1 mPNC-NLS interacts with MDM2. ITC plots demonstrate the interaction between MDM2 and mPNC-NLS. (A) The top panel exhibits successive titrations of the mPNC-NLS peptide (500 µM) into the MDM2 protein (50 µM) in phosphate buffer and the controlled heat of the peptide solution to the buffer is also performed (curves are offset for clarity). (B) The bottom plot demonstrates total number of injections considering dilution heats against the MDM2/mPNC-NLS molar ratio; the solid line defines the best-fitted curves to the "one set of binding sites" model. (C) Molecular docking image of only MDM2-p53 protein complex (PDB ID: 1YCR). (D) mPNC-NLS peptide targets and binds with MDM2 protein at its p53 transactivation domain with a binding energy of −6.3 kcal/mol.

antimycotics. Cultured cells (A549, WI38, and U87) were plated in 96-well plates at uniform density. Cell viability screening was done using varying (25 µM, 50 µM, 100 µM, and 200 µM) concentrations of peptide in DMEM medium after 24-h treatment.[20–22] MTT is widely popular as a colorimetric technique where the yellow tetrazole compound upon reduction by reductase enzymes present in viable cells converted to insoluble purple-colored formazan while the dead cells cannot interfere. A 1:1 DMSO/MeOH solvent was used to solubilize it further. Absorbance was recorded at 550 nm. Percentage viability has been calculated as $[(A_{550}$ Treated Cells $- A_{550}$ Background)/$(A_{550}$ Untreated Cells $- A_{550}$ Background)$] \times 100$.

2.8 | Apoptosis study

Human lung carcinoma cells: A549 ($\sim 5 \times 10^5$ cells/mL) were harvested in a six-well plate for 48 h. On the next day, a treatment concentration of 45 µM mPNC-NLS and mPNC was administrated for 24 h. Following the incubation period cells were treated with 100 µL of binding buffer solution containing propidium iodide (PI) along with Annexin V and incubated for an additional 15 min at 37°C. The fluorescence signal of annexin V and PI were analyzed at FITC and PI channels of the flow cytometer (BD LSRFortessa™) by employing emission filters at 530 and 610 nm, respectively. The populations of cells at Q1, Q2, and Q4 quadrants are considered necrotic, early, and late apoptosis, respectively, whereas Q3 quadrant cells are reckoned as a healthy cell population.

2.9 | Cell cycle analysis

A cell cycle analysis study has been accomplished by treatment in a similar way. A549 cells were treated with mPNC and mPNC-NLS separately at 45 µM concentration and incubated for 1 day. On the next day, cells were given a 45-min treatment of PI (100 µg/mL) and RNase (10 µg/mL) at 37°C temperature. At last, the cell cycle analysis was done by employing red channels of BD LSRFortessa™ flow cytometer with an emission filter at 610 nm.

2.10 | Cellular uptake study by fluorescence microscopic imaging

A549 cell suspension (500 µL) was plated on a glass bottom confocal dish at 1×10^3 density and cultured using 10% fetal bovine serum supplemented DMEM for 24 h. On the next day cells were washed with 1× PBS and treated with 5 µM carboxyfluorescein conjugated mPNC and mPNC-NLS containing serum-free colorless culture media and incubated for 4 h. After completion of the incubation period, the treatment containing media was discarded and cells were washed gently with 1× PBS. To stain the nucleus, cells were further treated with 1 µM Hoechst 33258 and incubated at 37°C for 1 h. Finally, cells were washed with 1× PBS and treated with fresh colorless serum-free DMEM. Live cells were imaged with an inverted fluorescence microscope at 40× objective (Olympus IX83) in DIC, FITC, and DAPI channels.

2.11 | Determination of cellular uptake by flow cytometry

In a six-well plate, A549 cells were plated at a density of 5×10^5 cells/well prior to 24 h of treatment. Next, the cells were treated with carboxyfluorescein-conjugated mPNC and mPNC-NLS peptides at 5 μM concentration and incubated for 4 h. At the end of 4 h, cells were washed with 1× PBS and trypsinized with 1× trypsin EDTA. The relative extent of cellular uptake of mPNC and mPNC-NLS peptides was measured by FACS ($E_{x\text{-wavelength}}$: 488 nm and $E_{m\text{-wavelength}}$: 500 to 600 nm) with respect to control A549 cells having no prior treatments.

2.12 | Cellular internalization study using FACS

The mechanism of cellular uptake of carboxyfluorescein-conjugated mPNC and mPNC-NLS treated cells was analyzed using the earlier reported method.[21] In summary, cultured A549 cells (1×10^5) were dislodged and replated in a serum-free colorless DMEM medium. Next, cells were incubated separately at 37°C and 4°C for 60 min and subsequent treatment of fluorescein-attached peptides at 5 μM concentration were employed and incubated at 37°C and 4°C for an additional 4 h. After the completion of the incubation period, the treatment media containing cells were centrifuged and excess fluorescein-mPNC and fluorescein-mPNC-NLS were removed from the solution and resuspended in a colorless DMEM culture medium with 1× trypsin and incubated for additional 15 min. Finally, cells were washed with 1× PBS and fluorescent signal was recorded at 568 nm channels using a BD LSRFortessa™ flow cytometer.

2.13 | The effect of mPNC and mPNC-NLS treatment on 3D multicellular spheroids

After completion of in vitro analysis, we were intrigued to check the effect of mPNC and mPNC-NLS on tumor environment mimicking 3D spheroid growth. To do this, we have employed a tumor-mimicking multicellular spheroid study developed with A549 cells.[23–25] Upon the formation of the spheroids on a 2% agarose-coated surface, separate treatments with mPNC and mPNC-NLS along with control were applied. The volume of the spheroids for untreated (control), mPNC, and mPNC-NLS treated ones were monitored for up to 7 days by using a 10× (Olympus IX83) microscope objective, and images were captured with an EMCCD camera starting from the day of treatment. Here, we have noted a gradual enhancement of volume for the spheroid of the untreated group due to the high proliferation of cancer cells, while remarkable repression of growth has been perceived for mPNC-NLS-treated multicellular spheroids. In conclusion, the above in vitro experiment surely explains that mPNC-NLS is a potential MDM2-targeting peptide.

2.14 | Western blot analysis to check the p53 and p21 expressions

To check the expression of p53 and p21 upon mPNC-NLS treatment we have performed Western blot analysis. A549 cells were cultured using DMEM + 10% FBS for 2 days in a humidified CO_2 incubator. Upon reaching confluency cells were dislodged from the tissue culture flask using 2 mL 1× trypsin–EDTA followed by 2-min incubation and gentle tapping. The cell suspension was collected with 4-mL media to neutralize the trypsin and centrifuged at 3000 rpm for 5 min. The collected pellets were then re-suspended into 6 mL fresh media and 500 μL of cell suspension was added to each well of two 6-well plates and incubated to reach sub-confluency. After 24-h incubation period, 45 μM mPNC-NLS treatment was added to each well, after 48 h of treatment the cells are scrapped using a sterile cell scraper. Collected cell suspension along with the media are taken into two 15-mL Falcon tubes and centrifuged at 300×*g*, 4°C for 5 min, the supernatant was discarded. 1 mL of PBS was added to cell pellets and centrifugation was performed two times resuspending in PBS (two times), using 300×*g* at 4° for 5 min; 200 μL of RIPA buffer containing 1% protease inhibitor was added to the pellet with simultaneous vortexing followed by 20 min incubation on ice. After the incubation, again vortexing had been done. Finally, the resultant solution was centrifuged for 20 min at 20,000×*g* at 4°C. The supernatant was collected in a fresh microcentrifuge tube and stored at −20°C temperature. Sodium dodecyl sulfate (SDS) polyacrylamide gel electrophoresis (PAGE) was performed with the isolated protein samples followed by transfer to a 0.45-μm PVDF (polyvinylidene difluoride) membrane with the help of a blot transfer unit. 5% BSA in 1× TBST was used to block the membrane for 2 h. After that, primary antibodies against p53, p21, and β-Actin were used to incubate the membrane at 4°C overnight. To remove backgrounds, the corresponding blot membrane was cleaned five times with 1× TBST buffer and incubated in the dark with HRP-conjugated anti-rabbit/anti-mouse secondary antibodies for 2 h at room temperature. Finally, 1× TBST buffer was used to wash the membrane five times and blots were developed by using a Luminata Forte Western HRP substrate. The amount of protein was subsequently quantified by using a Bradford reagent and a standard BSA plot. ImageJ software was used for the quantitative analyses of the blots to check the relative expressions of the blots represented as normalized to β-Actin.

3 | RESULTS AND DISCUSSION

At first, we synthesized QETFSDLWKLLVQRKRQKLMP (mPNC-NLS) and modified QETFSDLWKLL (mPNC) peptide and only VQRKRQKLMP (NLS). In this regard, it is important to mention that nuclear localizing signals are typically short and modular and can be added to protein/peptide sequences in a variety of ways (e.g., at the N- or C-terminus). To create our mPNC-NLS peptide, we first truncated the PNC-27 peptide at its N-terminus to obtain mPNC. Further

to keep the MDM2 binding activity of this modified PNC peptide (mPNC) unaffected, we decided to keep its N-terminus intact and uncrowded by incorporating our NLS at the C-terminus position. All these peptides (mPNC and mPNC-NLS) along with 5(6)-carboxyfluorescein attached (F-mPNC and F-mPNC-NLS) versions were synthesized by microwave-aided solid phase peptide synthesis (SPPS) procedure and further purified by C-18 reverse phase HPLC column with subsequent characterization with the aid of MALDI-TOF mass and NMR spectroscopy (only mPNC-NLS) (Figure S1–S6). As we know that the drug-receptor interaction plays a crucial role to unravel the biological impact of drugs in cells as well in animal models, such as cell proliferation, cytotoxicity, immune response, tumor metastasis, and drug delivery.[26] We were able to exhibit the potential interactions between our designed peptide (mPNC-NLS) and targeted protein (MDM2) through ITC experiment,[27–29] which leads us to perform various in vivo assays. Moreover, the isothermal titration calorimetric analysis demonstrates conspicuous receptor (MDM2)-ligand (mPNC-NLS) binding interaction upon the subtraction of heat of dilution (association constant, $K_a = (9.9 \pm 2.2) \times 10^4\ M^{-1}$) (Figure 1A,B). In addition to these, a molecular docking experiment with the designed m-PNC-NLS peptide and MDM2 protein (PDB: 1YCR) was performed to investigate its binding region. For this, we have chosen a p53 transactivation domain containing the MDM2 complex. Intriguingly, we have found that the designed mPNC-NLS peptide binds near the transactivation domain of p53 with a significantly higher binding affinity (binding energy: −6.3 kcal/mol) and interferes with the p53-MDM2 complexation (Figure 1C,D). From the literature study, it has been found that A549 (human lung cancer) cells contain overexpressed MDM2 protein, thus we have chosen A549 cells for our further cell-based in vitro studies.[15–18] Next, we were curious to check whether our modified PNC peptide (mPNC) along with its NLS-attached analog (mPNC-NLS) possesses cell penetrating as well as nuclear localizing aptitude or not. To check this, we have conjugated 5,6-carboxyfluorescein with mPNC and mPNC-NLS peptide, individually. A549 cells were incubated with fluorescein-conjugated mPNC-NLS and mPNC peptide for 4 h separately. Hoechst 33258 was used to stain the nucleus upon incubation for 1 h. Images were recorded with the aid of inverted fluorescence microscopy in DIC, FITC (488 nm), and DAPI (405 nm) channels respectively. Intriguingly, it has been noted that cells treated with F-mPNC-NLS (5 μM) exhibit significant nuclear localization whereas F-mPNC showed good cellular uptake but was unable to localize inside the nucleus (Figure 2A–H). Further, flow cytometry (FACS) analyses were done to scrutinize the cellular uptake phenomenon associated with mPNC and mPNC-NLS. FACS study reveals that at 5 μM concentration F-mPNC-NLS exhibited a significant internalization which can be attributed to the NLS sequence attached to mPNC (Figure 2I). Motivated by this observation, further we tried to inquire about the mechanistic pathways associated with the cellular uptake process via another flow cytometry analysis. To do this, two sets of cultured A549 cells were treated with F-mPNC-NLS peptide at 5 μM concentration and incubated separately at 37°C and 4°C for 1 h. Interestingly, FACS experimental results showed a higher uptake of F-mPNC-NLS into the A549 cells incubated at 37°C compared with 4°C. This result indicates that cellular uptake of F-mPNC-NLS proceeds mostly through the endocytosis pathway (Figure 3A). After performing a successful nuclear localization assay, we studied cell viability assay for both mPNC-NLS and mPNC peptides. In order to do this, treatments up to 200 μM concentrations for 24 h were employed on A549 cells. Interestingly, it has been observed that cells treated with mPNC-NLS exhibited effectively higher cytotoxicity [$IC50_{mPNC\text{-}NLS} = 44.9$ μM] compared with the cells treated with mPNC ($IC50_{mPNC} = 81.5$ μM) (Figure 3B). Additionally, we have performed a cell viability assay with another MDM2 positive cell line (U87 cells; glioblastoma) where we perceived that alike A549 cells mPNC-NLS showed higher cytotoxicity ($IC50_{mPNC\text{-}NLS} = 56.9$ μM) compared with mPNC peptide ($IC50_{mPNC} = 85.9$ μM) treatment (Figure S7). The cytotoxicity assay (A549 cells) demonstrated that the IC50 value of our designed mPNC-NLS peptide is 45 μM while the determined Kd value found in ITC experiment is 10 μM. However, it is important to mention that this distinction may arise due to the influx kinetics of peptides into the cell membrane, interaction of peptide with Pgp "housekeeping" proteins, peptide aggregation nature, and uptake of peptide drugs into the whole cells. As upon treatment with mPNC-NLS human lung carcinoma cells, that is, A549 exhibited significant cytotoxicity ($IC50 = 44.9$ μM) compared with glioblastoma cells, that is, U87 ($IC50 = 56.9$ μM), we have selected A549 cells for further future studies. Because mPNC-NLS interacts with the negative regulator of p53 protein (MDM2) and enhances the activity of p53, we were curious to check whether cell morphology and viability of the cells get affected by mPNC-NLS or not. The DIC image of A549 cells revealed a shrunken cellular morphology after 24-h treatment of 45-μM mPNC-NLS peptide treatment compared with the untreated cells, which indicates that mPNC-NLS promotes cytotoxicity probably via activation of apoptosis inducer p53 protein (Figures 3C and S8). A simultaneous LIVE/DEAD viability assay was performed with calcein AM and propidium iodide to check the effect of mPNC-NLS on cultured A549 cells. Upon cellular internalization, Calcein AM gets converted to green fluorescent dye calcein, which is an effective indicator of the viable cell whereas PI can only be internalized through a compromised cell membrane and exhibits its red fluorescence upon intercalating with DNA. The fluorescence microscopic images of the mPNC-NLS (45 μM) treated cells exhibit a significantly higher amount of red fluorescent PI stained cells along with fewer green fluorescent calcein positive cells as compared with the control, which further substantializes our earlier MTT result (Figure S9). Interestingly, it has been observed that mPNC-NLS peptide remained non-cytotoxic toward the normal lung fibroblast cells (WI38 cells) even up to 200-μM treatment of mPNC-NLS for 24 h (Figures 3D and S9(d)). These in sum indicate that due to the lack of membrane-residing MDM2 protein expression, mPNC attached to NLS was unable to bind at its target site (MDM2 protein). Being assured of the cytotoxic nature of mPNC-NLS in MDM2 positive cells, we have performed the cell cycle assay upon treatment with mPNC-NLS (45 μM) via flow cytometric analysis using PI to stain DNA quantitatively. From the FACS data, we have concluded that mPNC-NLS effectuates cell cycle arrest at the G2/M phase followed

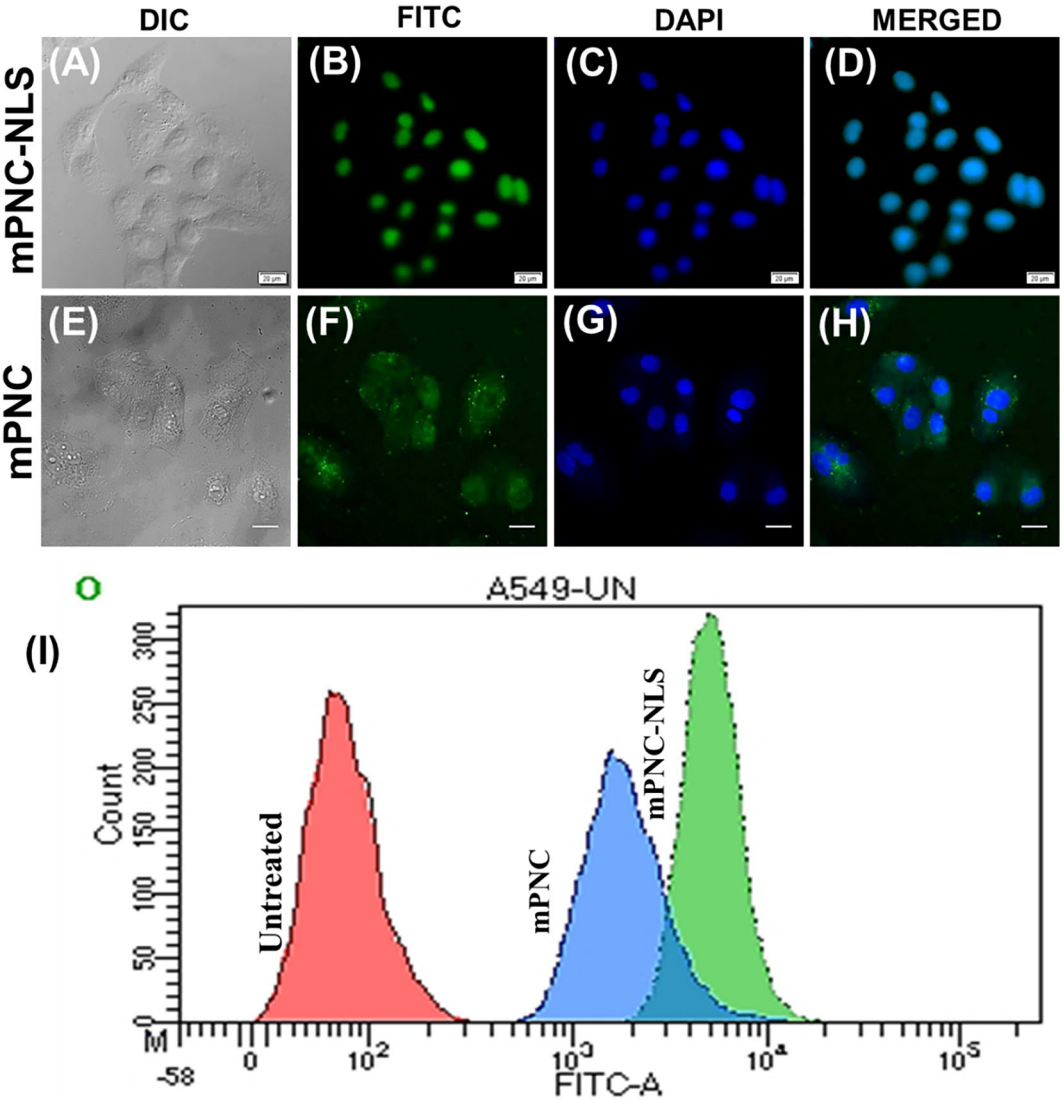

FIGURE 2 Cellular uptake of fluorescein-tagged peptides. Microscopic images were recorded in DIC mode, FITC (488 nm), and DAPI (405 nm) channels. Extreme right images are merged images of 405 nm and 488 nm. A merged image of F-mPNC-NLS (5 μM) indicates significant nuclear co-localization while F-mPNC exhibits good cellular uptake (A–H). Scale bars correlated to 20 μm. (I) The flow cytometric analysis explains the higher uptake of mPNC- NLS compared with mPNC (5 μM) after treatment with A549 cells for 4 h at 37°C.

by apoptotic cell death (Figure 4A–D). Further ratification of cellular response was confirmed by flow cytometric (FACS) analysis with the help of Annexin V/PI in A549 cells. From the quantified experimental data of cell death, we concluded a significantly higher cell population at simultaneous early and late phases of apoptosis, suggesting the initiation of apoptotic cell death upon treatment of mPNC-NLS (Figure 5A–D). After that, we demonstrated the subsequent elevation of the expression of p53 and p21 proteins using both immunocytochemistry and Western blot analysis. The observed merged color (Pink alike) raised from the cell nucleus indicates the activation of p53 as well as p21 protein after treatment with mPNC-NLS (45 μm). Intriguingly this expression was found to be higher in mPNC-NLS-treated A549 cells compared with untreated cells after 24 h (Figures S10 and S11). A similar observation was reflected in the protein immunoblot assay where an increased expression of both p53 and p21 proteins are apparent in mPNC-NLS treated cells as compared with control (Figure S12). Finally, we have validated the effect of mPNC-NLS on tumor-impersonating multicellular 3D spheroid formed of A549 cells.[14,15,20] Stem cell-like multicellular 3D (spheroids) cells were cultured on a 35 mm glass bottom confocal dish previously coated with 1% agarose. Initially, the tumor penetration ability of mPNC-NLS has been studied using 3D spheroid of A549 cells. 3D spheroids formed from A549 cells were treated with F-mPNC-NLS and to counterstain the nucleus Hoechst 33258 was used. Fluorescence microscopic images reveal a uniform penetration and distribution of F-mPNC-NLS all around the spheroid along with the core region of it too (Figure 6A–D). It indicates that F-mPNC-NLS (5 μM) can invade both 2D monolayer cells as well as the 3D spheroid of A549 cells significantly. The significant spheroid penetration ability of F-mPNC-NLS motivated us to study its effect on 3D spheroid

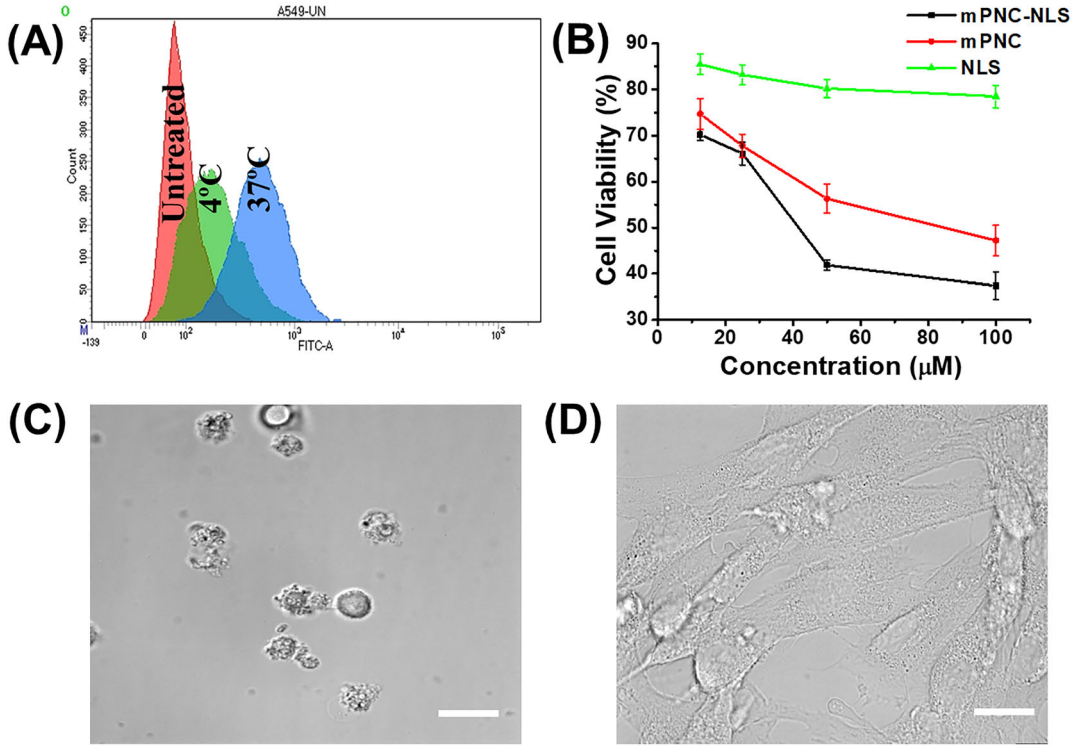

FIGURE 3 (A) mPNC-NLS uptake undergoes through endocytosis pathway, (B) cell viability study indicates that mPNC-NLS exhibited higher cytotoxicity compared with mPNC and NLS along, (C) DIC image of A549 cells indicate that mPNC-NLS treatment (45 μM) affects the cell morphology and kills the A549 cells significantly whereas it does not affect (D) normal fibroblast (WI38) cells. The scale bar corresponds to 20 μm.

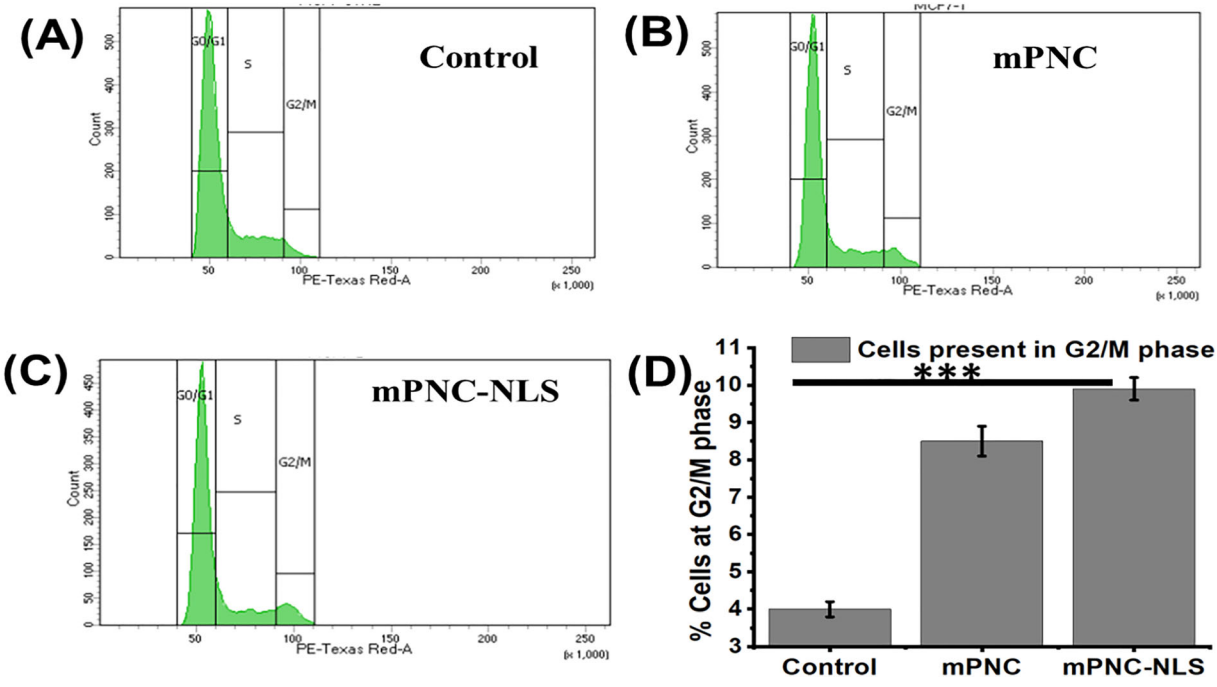

FIGURE 4 Comparative cell cycle study performed in mPNC-NLS and mPNC peptide indicating higher amount cell arrest undergoes at G2/M phase (A–D). Results were demonstrated as mean ± SD. In all cases, $*p < 0.05$ was considered an indicator of a significant difference. The asterisk denotes statistically significant differences between indicated classes: ns $p > 0.05$, $***p < 0.001$, $****p < 0.0001$.

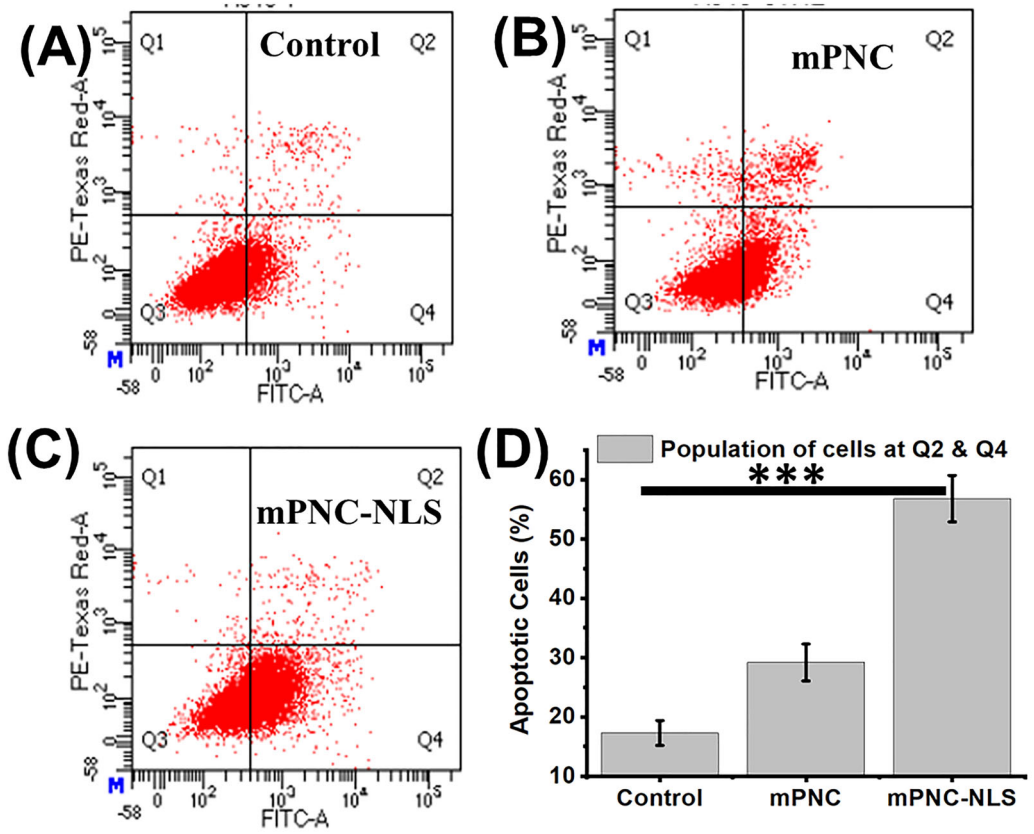

FIGURE 5 Comparative apoptosis study performed in mPNC-NLS and mPNC peptide indicating higher amount apoptotic cell death (early and late) compared with mPNC at 45-μM concentration (A–D). Results were demonstrated as mean ± SD. In all cases, $^{*}p < 0.05$ was considered an indicator of a significant difference. The asterisk denotes statistically significant differences between indicated classes: ns $p > 0.05$, $^{***}p < 0.001$, $^{****}p < 0.0001$.

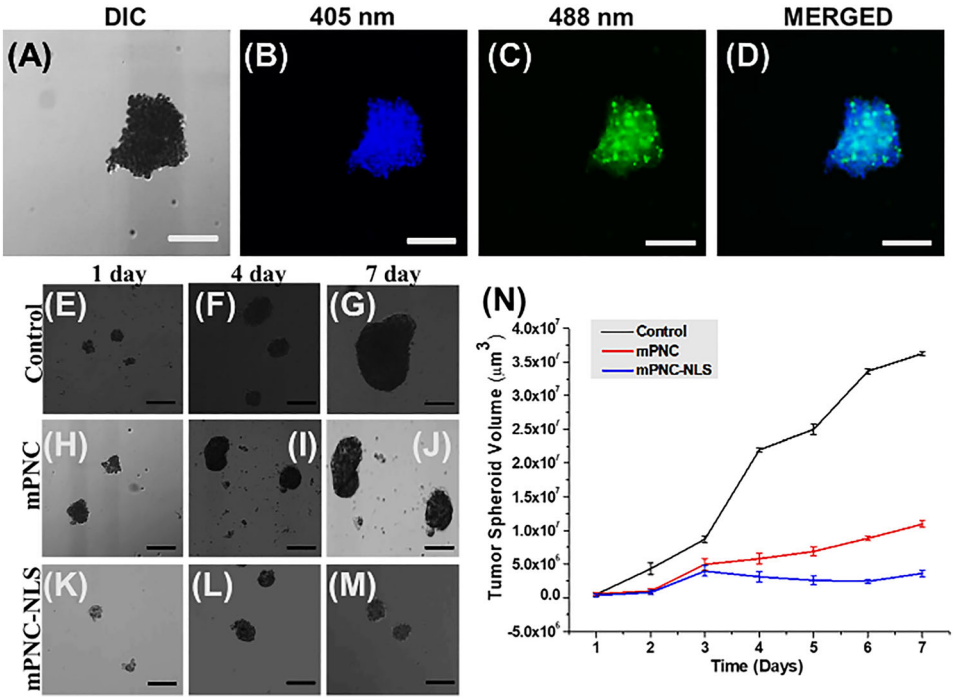

FIGURE 6 Ingression of F-mPNC-NLS treatment inside the spheroids formed by A549 cells observed in DIC image (A), Hoechst 33258 (B), F-mPNC-NLS (C), and merged image (D). Comparative spheroid growth inhibition study of untreated (E–G), mPNC (H–J), mPNC-NLS (K–M) treated cells up to 7 days. Scale bars correspond to 100 μm. Graphical representation exhibits a significant inhibition of tumor spheroid growth after treatment of mPNC-NLS compared with untreated and mPNC (N).

growth upon treatment. A tumor-mimicking spheroid growth inhibition analysis has been performed following the earlier reported method.[20,21] At the end of 5 days of spheroid growth, all the spheroids were treated with 45 μM of mPNC-NLS. Both untreated and mPNC-NLS-treated spheroid growth was monitored using an inverted microscope with a Z stack feature. The dimension of the spheroid was monitored and quantified for up to 7 days, from the day of the treatment. From the quantitative evaluation as well as microscopic images we observed a significant enhancement of tumor spheroids of the untreated group, while effective growth inhibition was reflected from mPNC-NLS treated spheroid (Figure 6E–N). It is interesting to conclude that this MDM2-targeted mPNC-NLS peptide can impart a marked tumor spheroid growth inhibitory effect for up to 7 days.

4 | CONCLUSION

Attenuation of MDM2-p53 protein–protein interaction is an effective way to trigger the induction of p53 mediated apoptosis pathway in tumor cells. In this regard, peptide-based anticancer therapeutics are quite effective due to their higher selectivity and significant biocompatibility. In this research work, we have rationally designed and developed a novel peptide containing both nuclear localizing and MDM2 binding counterpart that targets the nuclear MDM2 protein, effectively activates the p53 protein, and exhibits effective toxicity (IC50 = 45 μM) toward the A549 and U87 cancer cells. By flow cytometry and fluorescence microscopic images, we have further established that this synthesized multi-domain mPNC-NLS peptide undergoes rapid cellular internalization via endocytic pathways and subsequently localizes inside the nucleus. Intriguingly, the designed mPNC-NLS peptide remains non-cytotoxic to MDM2-negative normal cells (WI38) which further materializes its future in vivo therapeutic prospect. Further molecular docking analysis, isothermal calorimetry results, substantiate the fact that mPNC-NLS has a significant binding affinity toward the MDM2 protein. Immunocytochemistry, as well as immunoblotting analysis results, show that mPNC-NLS induces apoptotic death of lung cancer cells by activation of p53 and p21 proteins and remarkably stifled the in vitro growth of 3D spheroids composed of A549 cells. In conclusion, our results suggest mPNC-NLS peptide-mediated increase in p53 activity via disruption of MDM2/p53 interaction may have better future therapeutic application for the treatment of the MDM2 overexpressing cancer cells.

5 | ASSOCIATED CONTENT

Supporting Information contains HPLC-chromatogram and mass spectrum of mPNC-NLS, ^{1}H NMR of mPNC-NLS peptide, HPLC-chromatogram and mass spectrum of mPNC, HPLC-chromatogram and mass spectrum of fluorescein attached mPNC-NLS, HPLC-chromatogram and mass spectrum of fluorescein attached mPNC, HPLC-chromatogram and MALDI mass spectrum of nuclear localizing sequence (NLS), comparative cell viability study (mPNC-NLS, mPNC and NLS) performed in glioblastoma (U87) cells up to 100 μM concentration for 24 comparative cell morphology study performed in A549 cells, fluorescence microscopic images of LIVE/DEAD analysis in A549 cells upon treatment with mPNC-NLS, fluorescence microscopic images revealing the activation of p53 protein in A549 cells upon treatment with mPNC-NLS, fluorescence microscopic images reveal the activation of p21 protein in A549 cells upon treatment with mPNC-NLS, Western blot expression of p53 and p21 protein in A549 cells upon treatment with mPNC-NLS as compared with control, quantitative calculation for the relative expressions of p53 and p21.

ACKNOWLEDGMENTS

The authors express their gratitude to NCCS-Pune for the cell lines. NM thanks MHRD and IIT Jodhpur Smart Healthcare for her fellowship, DB thanks DST Inspire, PM and PKG thank CSIR, and SB acknowledges ICMR-RA fellowship (45/35/2022-DDI/BMS). SG kindly acknowledges SERB India (STR/2020/000048) and the IIT Jodhpur SEED grant for financial assistance.

CONFLICT OF INTEREST STATEMENT

There are no conflicts of interest declared.

DATA AVAILABILITY STATEMENT

The data underlying this study are available in the published article and the online Supporting Information.

ORCID

Prasenjit Mondal https://orcid.org/0000-0003-0767-449X
Surajit Ghosh https://orcid.org/0000-0002-8203-8613

REFERENCES

1. Bieging KT, Mello SS, Attardi LD. Unravelling mechanisms of p53-mediated tumour suppression. *Nat Rev Cancer*. 2014;14(5):359-370. doi:10.1038/nrc3711
2. Hu W, Feng Z, Teresky AK, Levine AJ. p53 regulates maternal reproduction through LIF. *Nature*. 2007;450(7170):721-724. doi:10.1038/nature05993
3. Giaccia AJ, Kastan MB. The complexity of p53 modulation: emerging patterns from divergent signals. *Genes Dev*. 1998;12(19):2973-2983. doi:10.1101/gad.12.19.2973
4. Hu W, Feng Z, Levine AJ. The regulation of multiple p53 stress responses is mediated through MDM2. *Genes Cancer*. 2012;3(3-4):199-208. doi:10.1177/1947601912454734
5. Vousden KH, Prives C. Blinded by the light: the growing complexity of p53. *Cell*. 2009;137(3):413-431. doi:10.1016/j.cell.2009.04.037
6. Guo XE, Ngo B, Modrek AS, Lee W. Targeting tumor suppressor networks for cancer therapeutics. *Curr Drug Targets*. 2014;15(1):2-16. doi:10.2174/1389450114666140106095151
7. Issaeva N, Bozko P, Enge M, et al. Small molecule RITA binds to p53, blocks p53–HDM-2 interaction and activates p53 function in tumors. *Nat Med*. 2004;10(12):1321-1328. doi:10.1038/nm1146
8. Ndagi U, Mhlongo N, Soliman ME. Metal complexes in cancer therapy—an update from drug design perspective. *Drug Des Devel Ther*. 2017;11:599-616. doi:10.2147/DDDT.S119488
9. Hoelder S, Clarke PA, Workman P. Discovery of small molecule cancer drugs: successes, challenges and opportunities. *Mol Oncol*. 2012;6(2):155-176. doi:10.1016/j.molonc.2012.02.004

10. Li F, Li N, Li LL, Wang T. One step quantum key distribution based on EPR entanglement. *Sci Rep*. 2016;6(1):28767. doi:10.1038/srep28767
11. Lin R, Shi Ng L, Wang C. In vitro study of anticancer drug doxorubicin in PLGA-based microparticles. *Biomaterials*. 2005;26(21):4476-4485. doi:10.1016/j.biomaterials.2004.11.014
12. Mukherjee N, Roy R, Ghosh S, Ghosh S. Self-assembled antimitotic peptide vesicle designed from α,β-tubulin heterodimer Interface for anticancer drug delivery. *Israel J Chem*. 2022;62(9–10):e202200019. doi:10.1002/ijch.202200019
13. Jana B, Barman S, Roy R, et al. Fluorine substituted proline enhances the tubulin binding potential of a tetrapeptide at the GTP binding pocket causing the inhibition of microtubule motility and an antimitotic effect. *J Phys Chem B*. 2021;125(31):8768-8780. doi:10.1021/acs.jpcb.1c04323
14. Adak A, Das G, Gupta V, et al. Evolution of potential antimitotic stapled peptides from multiple helical peptide stretches of the tubulin heterodimer interface: helix-mimicking stapled peptide tubulin inhibitors. *J Med Chem*. 2022;65(20):13866-13878. doi:10.1021/acs.jmedchem.2c01116
15. Mondal P, Mohapatra S, Bhunia D, et al. Designed hybrid anticancer nuclear-localized peptide inhibits aggressive cancer cell proliferation. *RSC Med Chem*. 2022;13(2):196-201. doi:10.1039/D1MD00324K
16. Jagot-Lacoussiere L, Kotula E, Villoutreix BO, Bruzzoni-Giovanelli H, Poyet JL. A cell-penetrating peptide targeting AAC-11 specifically induces cancer cells death. *Cancer Res*. 2016;76(18):5479-5490. doi:10.1158/0008-5472.CAN-16-0302
17. Sarafraz-Yazdi E, Bowneb WB, Adlerc V, et al. Anticancer peptide PNC-27 adopts an HDM-2-binding conformation and kills cancer cells by binding to HDM-2 in their membranes. *Proc Natl Acad Sci U S A*. 2010;107(5):1918-1923. doi:10.1073/pnas.0909364107
18. Davitt K, Babcock BD, Fenelus M, et al. The anti-cancer peptide, PNC-27, induces tumor cell necrosis of a poorly differentiated non-solid tissue human leukemia cell line that depends on expression of HDM-2 in the plasma membrane of these cells. *Ann Clin Lab Sci*. 2014;44(3):241-248.
19. Kussie PH, Gorina S, Marechal V, et al. Structure of the MDM2 oncoprotein bound to the p53 tumor suppressor transactivation domain. *Science*. 1996;274(5289):948-953. doi:10.1126/science.274.5289.948
20. Bhunia D, Pradhan K, Das G, Ghosh S, Mondal P, Ghosh S. Matrix metalloproteinase targeted peptide vesicles for delivering anticancer drugs. *Chem Commun*. 2018;54(67):9309-9312. doi:10.1039/C8CC05687K
21. Chatterjee S, Suresh Kumar G. Small molecule induced poly(A) single strand to self-structure conformational switching: evidence for the prominent role of H-bonding interactions. *Mol Biosyst*. 2017;13(5):1000-1009. doi:10.1039/C7MB00031F
22. Brogan AP, Widger WR, Bensadek D, Riba-Garcia I, Gaskell SJ, Kohn H. Development of a technique to determine bicyclomycin-rho binding and stoichiometry by isothermal titration calorimetry and mass spectrometry. *J Am Chem Soc*. 2005;127(8):2741-2751. doi:10.1021/ja046441q
23. das A, Chatterjee S, Suresh Kumar G. Targeting human telomeric G-quadruplex DNA with antitumour natural alkaloid aristololactam-β-D-glucoside and its comparison with daunomycin. *J Mol Recognit*. 2017;30(10):e2639. doi:10.1002/jmr.2639
24. Bhunia D, Mohapatra S, Kurkute P, et al. Novel tubulin-targeted cell penetrating antimitotic octapeptide. *Chem Commun*. 2016;52(85):12657-12660. doi:10.1039/C6CC05110C
25. Bhunia D, Mondal P, Das G, et al. Spatial position regulates power of tryptophan: discovery of a major-groove-specific nuclear-localizing, cell-penetrating tetrapeptide. *J Am Chem Soc*. 2018;140(5):1697-1714. doi:10.1021/jacs.7b10254
26. Ma W, Yang L, He L. Overview of the detection methods for equilibrium dissociation constant KD of drug-receptor interaction. *J Pharm Anal*. 2018;8(3):147-152. doi:10.1016/j.jpha.2018.05.001
27. Zamek-Gliszczynski MJ, Lee CA, Poirier A, et al. Galetin and international transporter consortium. *Clin Pharmacol Ther*. 2013;94(1):64-79. doi:10.1038/clpt.2013.45
28. Hoffmeyer S, Burk O, von Richter O, et al. Functional polymorphisms of the human multidrug-resistance gene: multiple sequence variations and correlation of one allele with P-glycoprotein expression and activity in vivo. *PNAS Nexus*. 2000;97(7):3473-3478. doi:10.1073/pnas.97.7.3473
29. Bai D, Zhang J, Xiao W, Zheng X. Regulation of the HDM2-p53 pathway by ribosomal protein L6 in response to ribosomal stress. *Nucleic Acids Res*. 2014;42(3):1799-1811. doi:10.1093/nar/gkt971

SUPPORTING INFORMATION

Additional supporting information can be found online in the Supporting Information section at the end of this article.

How to cite this article: Mukherjee N, Bhunia D, Garai PK, Mondal P, Barman S, Ghosh S. Designed novel nuclear localizing anticancer peptide targets p53 negative regulator MDM2 protein. *J Pept Sci*. 2024;30(1):e3535. doi:10.1002/psc.3535